Computing the viscosity of supercooled liquids. II. Silica and strong-fragile crossover behavior

Akihiro Kushima,[1,a)] Xi Lin,[2,b)] Ju Li,[3] Xiaofeng Qian,[1] Jacob Eapen,[4] John C. Mauro,[5] Phong Diep,[5] and Sidney Yip[1,b)]

[1]*Department of Nuclear Science and Engineering and Department of Materials Science and Engineering, Massachusetts Institute of Technology, Cambridge, Massachusetts 02139, USA*
[2]*Department of Mechanical Engineering and Division of Materials Science and Engineering, Boston University, Boston, Massachusetts 02215, USA*
[3]*Department of Materials Science and Engineering, University of Pennsylvania, Philadelphia, Pennsylvania 19104, USA*
[4]*Department of Nuclear Engineering, North Carolina State University, Raleigh, North Carolina 27695, USA*
[5]*Science and Technology Division, Corning Incorporated, Corning, New York 14831, USA*

A recently developed atomistic method capable of calculating the fragile (non-Arrhenius) temperature behavior of highly viscous liquids is further tested by studying a model of SiO_2, a glass former well known for its Arrhenius temperature behavior (strong). The method predicts an Arrhenius temperature variation, in agreement with experiments, the origin of which is revealed by both quantitative and qualitative results on transition state pathways, activation barrier analysis, energy landscape connectivity, and atomistic activation mechanisms. Also predicted is a transition from fragile to strong behavior at a lower viscosity, below the range of measurements, which had been previously suggested on the basis of molecular dynamics simulations. By systematically comparing our findings with corresponding results on the binary Lennard-Jones system (fragile) we gain new insights into the topographical features of the potential energy landscape, characteristics that distinguish strong from fragile glassy systems. We interpret fragility as a universal manifestation of slowing of dynamics when the system becomes trapped in deep energy basins. As a consequence, all glass-forming systems, when cooled from their normal liquid state, should exhibit two transitions in temperature scaling of the viscosity, a strong-to-fragile crossover followed by a second transition reverting back to strong behavior. © *2009 American Institute of Physics.* [doi:10.1063/1.3243854]

I. INTRODUCTION

Despite an abundance of data on the viscosity of many liquids in an undercooled state, understanding the observed temperature variations at the microscopic level remains incomplete.[1–3] The challenge, as is well known, is that with measurements spanning more than ten orders of magnitude, no atomistic methods yet exist that can deal with dynamical relaxations over the entire temporal range. Recently we proposed a method to investigate the transition state pathways (TSPs) of a liquid system of particles that has been rapidly cooled.[4] Using this approach to deduce an effective temperature-dependent activation barrier, we were able to describe the essential features of the viscosity of fragile glass formers, without input from experiments. Our results provided explicit details to explain the characteristic non-Arrhenius variation with temperature; they also bring out the combined role of thermodynamics, through the concept of inherent structure of liquids, and activated state kinetics, based on TSP trajectories. Because this study[4] was focused on the binary Lennard-Jones (BLJ) potential model, an inter-

atomic interaction that does not correspond to any real material, a next step would be to test the approach on a system where direct comparison with experiment can be made. Here we present a study of SiO_2 for which the measured viscosity is well known to follow closely an Arrhenius temperature variation. We find that the calculations match very well with the experiments; moreover, comparing quantitative results between a strong (SiO_2) and a fragile (BLJ) glass former allows us to clarify the features of the potential energy landscape that characterize fragile versus strong behavior,[5] as well as to provide further evidence for the existence of universal crossover behavior in all supercooled liquids.[3,6]

II. DETERMINATION OF EFFECTIVE ACTIVATION BARRIER

The procedure we have developed to compute the viscosity of supercooled liquids has been described in detail previously in the study of a fragile system using the binary Lennard-Jones interatomic potential.[4] The same method is now applied to SiO_2 for which we adopt a relatively simple potential that does not involve explicit Coulomb interactions.[7] We use a periodic simulation cell containing 256 atoms at a density of 2210 kg/m^3.[8] With the Si and O particles placed randomly, constant-temperature molecular

a)Electronic mail: kushima@mit.edu.
b)Authors to whom correspondence should be addressed. Electronic mail: linx@bu.edu and syip@mit.edu.
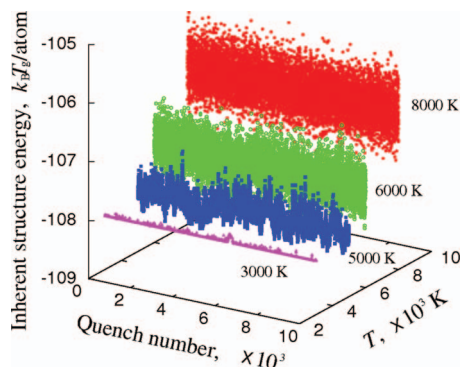
FIG. 1. Inherent structure spectra obtained by steepest descent quench at the indicated temperatures. Each constant-temperature MD simulation run consists of 10^8 steps of 3.0 fs. Each distribution involves 10^4 quenches, carried out at intervals of 10^4 steps. Energy unit is $k_B T_g$ with $T_g = 1580$ K.

dynamics (MD) simulations are performed starting at 20 000 K and cooling down to 500 K at a rate of 10^{14} K/s. At several temperatures along the way, long simulation runs (10^8 MD steps) are made to obtain trajectories from which steepest descent energy minimizations are carried out at intervals of 10^4 steps, thus obtaining an ensemble of energy-minimum states, the so-called inherent structures,[9] and their corresponding atomic configurations. Four such ensembles, which we denote by the index $\{\alpha\}$, are shown in Fig. 1. Each ensemble is a collection of 10^4 relaxed energies $\{E(\alpha)\}$ obtained by minimization at the indicated temperatures.

Before proceeding we comment on the choice of energy unit that we will adopt to express the various results in this study. In atomistic calculations, it is conventional to express all energies in units of an energy parameter that characterizes the interatomic potential, such as the well depth in a Lennard-Jones potential. Since our SiO_2 potential does not have such a convenient parameter, we could simply use absolute units for the energies. However, because we are interested in the temperature dependence of the shear viscosity $\eta(T)$ of glassy liquids, we decided to use the glass transition temperature T_g, defined operationally by $\eta(T_g) = 10^{12}$ Pa s, as the energy unit (more precisely, $k_B T_g$, where k_B is Boltzmann constant). This choice may seem inconvenient to the reader, at least until we explain how our method enables T_g to be determined; however, its advantage becomes apparent when one realizes that in the discussions to follow, it is natural to scale all temperatures relative to T_g. This scaling is also useful for comparing the two prototypical strong and fragile systems, SiO_2 and BLJ.

It is seen in Fig. 1 that the spectrum of relaxed energies $\{E(\alpha)\}$ generally narrows as the quench temperature is lowered. In particular, the sharp narrowing occurring when temperature drops from 5000 K to 3000 K signals the system has become effectively frozen on the time scale of the simulation. This also indicates that it would be computationally inefficient to continue probing the inherent structure at these low temperatures. We therefore turn to a description of inherent structure in terms of a quench probability distribution $f(E|T)$.[10] We first construct a reference distribution using the direct simulation data at 5000 K, and obtain distributions for all lower temperatures by the scaling property of $f(E|T)$.
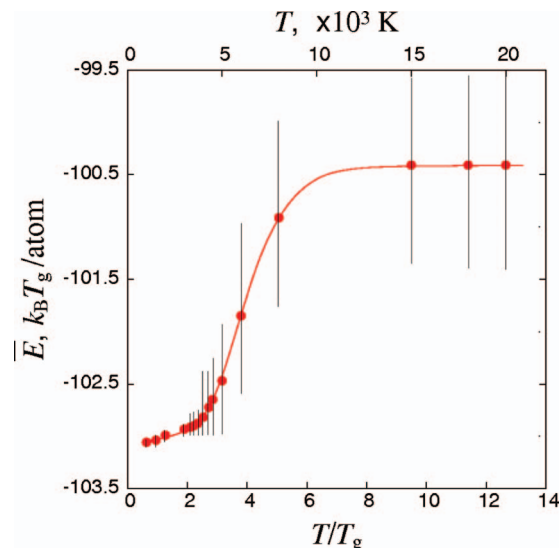

FIG. 2. Temperature variation of average inherent structure energy of the SiO_2 model (circles) obtained according to Eq. (1). The vertical line indicates the range of the quenched energy distribution at each T. Solid line is a fitted curve through the MD simulation data points.

The reason inherent structure spectra at low temperatures are of interest is that we would like to continue probing the system when direct MD can no longer handle the slow dynamics. More specifically, we will associate the ensemble of inherent structures at a given temperature T by an average energy $\bar{E}$, which is temperature dependent,

$$\bar{E}(T) = \int E(\alpha) f(E|T) dE. \tag{1}$$

The variation of $\bar{E}$ with T computed using MD results at 5000 K and above, and quench probability distributions obtained in the above manner at lower temperatures, is shown in Fig. 2. We indicate in the figure the range of the quench probability distribution $f(E|T)$ at each T. One sees clearly the dramatic narrowing of the energy distribution as temperature is lowered to $2T_g$. We interpret $\bar{E}$ as an effective (coarse-grained) energy minimum, a measure of the potential well depth that the system sees on the average at temperature T. Then what Fig. 2 shows is that at high temperatures the well is shallow and essentially constant, but when the temperature is lowered past a certain threshold (in this case $\sim 6T_g$) the well depth increases sharply, meaning a significant change in the energy landscape. This behavior of the inherent structure is quite general, for example, it is clearly seen in the case of the binary Lennard-Jones system.[4,11]

The essence of our method lies in applying a basin filling procedure to generate TSP trajectories.[4] The resulting trajectories, obtained from three initial conditions, each with the system in a different energy-minimum state, are shown in Fig. 3. Trajectory (a) is generated by starting at a relatively high energy minimum chosen from the inherent structure distribution produced by quenching at 8000 K. The system is seen to readily follow an energy-lowering path to explore regions of lower energies. In contrast, trajectory (c) starts from an initial state that is low in energy, and during the sampling the system continues to explore the low-energy
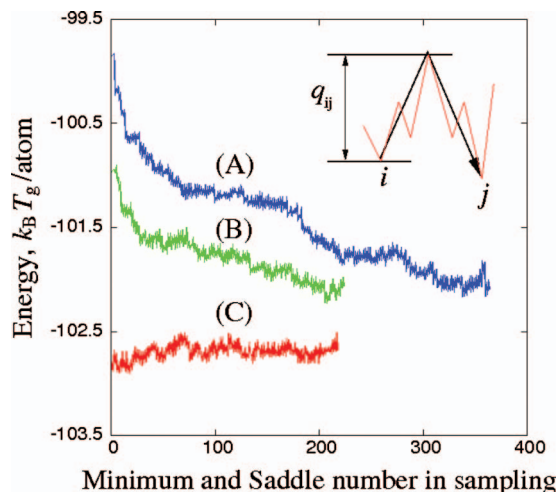
FIG. 3. TSP trajectories generated by the basin filling algorithm (Ref. 4), each starting at inherent structure states taken from three distributions in Fig. 1, (a) 8000 K, (b) 6000 K, and (c) 3000 K, respectively. The inset shows the activation energy linking local energy minima i and j.

FIG. 4. (a) Scatter plot of values q_{ij} extracted from the trajectory labeled as (a) in Fig. 3. A point is shown for each minimum i and all j that can be connected by an activation barrier q_{ij}. (b) Distributions of activation barriers at three selected energy minima, denoted as 1, 2, and 3 in (a).

landscape. We also observe that all three trajectories exhibit local energy fluctuations of similar magnitude. This is a feature that we will comment on further in discussing the potential energy surface (PES) topography of strong versus fragile systems.

Each TSP trajectory is an alternating sequence of local energy minimum and saddle point energy. Each energy minimum is the result of a series of energy-penalty activation and full-system relaxation, and each saddle point is found by backprojection.[4] A particular trajectory therefore delineates a pathway that the system follows as it explores the PES. Because the energy-penalty functions are not removed once they are imposed, they effectively modify the PES as the sampling proceeds. In this respect, we are not dealing with a static potential energy landscape. The landscape associated with our trajectories is being continuously modified as part of the sampling process, as a form of activation-relaxation feedback. For any single trajectory (sampling), the information pertaining to systemwide behavior as well as the individual particle rearrangements during each activation-relaxation step are fully retained. With these data one can perform a statistical analysis to extract an effective (coarse-grained) activation barrier for structural relaxation at the given temperature.[4] We begin by considering the amount of minimal activation energy q_{ij} required to climb out of a local minimum (initial state i) and surmount all the intermediate barriers necessary to reach another local minimum (final state j). See the inset of Fig. 3. Since different pairs of (i,j) may have the same value of activation energy, we show in Fig. 4(a) along the ordinate the magnitude of the activation barrier $Q=q_{ij}$ for all possible j states paired with various i states (along the abscissa) selected from the TSP trajectory labeled as (a) in Fig. 3. We can see that for an initial state at high energy (climbing out of shallow wells), only a few low-energy activation barriers are sampled, meaning that it is relatively easy for the system to climb out of shallow wells. On the other hand, for initial states at low E_i many transitions are sampled spanning over a wide range of activation
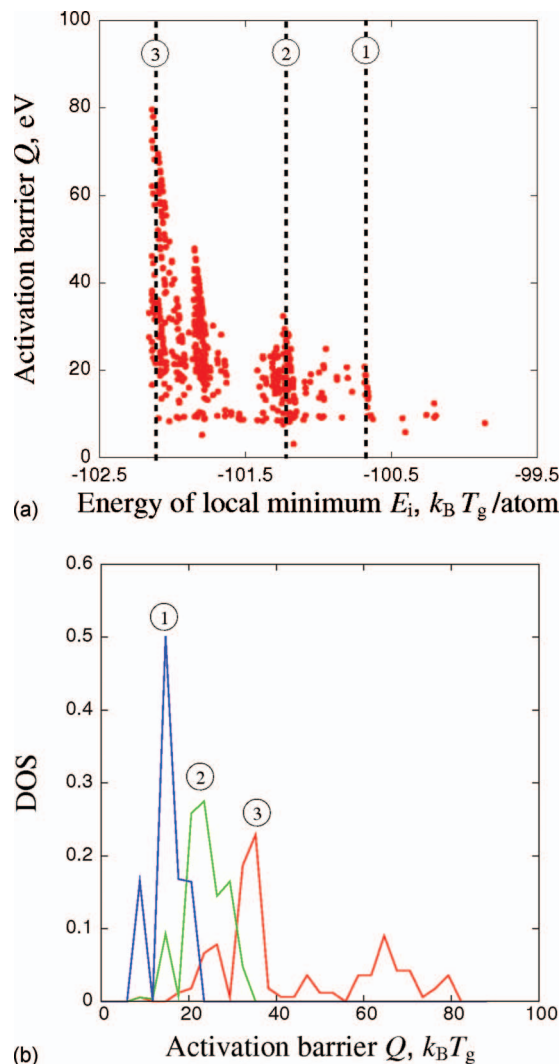
barriers. Not all the barriers sampled are seen in Fig. 4(a) because of data points falling on top of each other. For details of the density distribution of sampled barriers we show in Fig. 4(b) distributions for three selected values of E_i, indicated along the ordinate in Fig. 4(a); they correspond to initial states lying in a shallow well, an intermediate case, and the deepest well we have sampled. All three distributions are seen in Fig. 4(b) to be rather sharply peaked, except there seems to be a tail extending to quite high Q values in the case of the deepest well. If we consider only the most frequently occurring Q-values, peaks of the distribution, we obtain a correlation between activation barrier Q and the initial energy of the trajectory sampling E_i, shown in Fig. 5(a). In what follows we will call this the single activation path (SAP) approximation. Keeping in mind that low E_i values correspond to deep wells, we see that our approximation leads to an activation barrier that starts at low energies for shallow wells, rises sharply when the wells become deep, and levels off to a constant value for the deepest wells. This
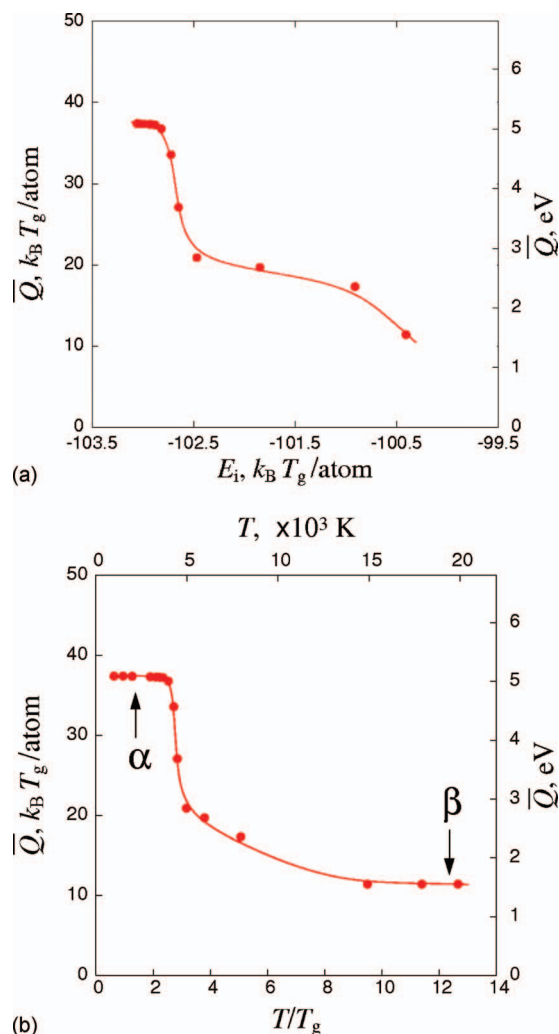
FIG. 5. (a) Correlation of effective activation barrier with well depth, result of SAP approximation. (b) Variation of effective activation barrier with quench temperature obtained by two coarse-graining steps (see text). High and low activation barriers, where atomic configurations associated with activation processes will be examined, are indicated by α and β, respectively.

is the essential information given by the combination of our activation-relaxation basin filling algorithm and statistical activation barrier analysis.

To apply the foregoing microscale analysis to describe system behavior on the macroscale, we need to incorporate the information concerning the temperature variation of the average inherent structure energy (well depth). Thus we combine Fig. 5(a) with Fig. 2 to obtain an effective (coarse-grained) temperature-dependent activation barrier, shown in Fig. 5(b). The mapping process in going from Fig. 5(a) to Fig. 5(b) involves two distinct steps, $\bar{Q}(E_i) \equiv \bar{Q}(\bar{E}) \equiv \bar{Q}(T)$.

In the first step E_i is replaced by the average inherent structure energy $\bar{E}$, with $\bar{Q}$ denoting a coarse-grained quantity. In the second step we make use of the correlation between $\bar{E}$ and T previously displayed in Fig. 2. It is worthwhile to emphasize again a certain temperature variation that is seen in Fig. 5(b). For the strong glass-former system under consideration the effective barrier is temperature insensitive

for T above $\sim 10T_g$. Below this range the barrier increases sharply until T reaches $\sim 3.5T_g$, where it abruptly levels off and stays constant.

III. VISCOSITY OF SILICA: THEORY AND EXPERIMENTS

The linear response theory description of viscosity is based on the general Green–Kubo formalism,[12,13] where transport coefficients are expressed as the integral of appropriate time correlation functions. In the case of shear viscosity the shear stress autocorrelation function can be computed by MD simulation once the interatomic potential is given. This approach is well validated when the viscosity value is not too large, $\eta \leq 10^{-4}$ Pa s.[14] For the high-viscosity region of most interest in this study, MD becomes ineffective because of the slow relaxation of the stress correlation function. Thus there are essentially no atomistic calculations of viscosity beyond about 10^2 Pa s.[15] In the case of silica, this is somewhat below the range where experimental measurements have been made.[16] As an alternative to MD simulations we recently proposed a method to calculate $\eta(T)$ using the TSP trajectory generated by the basin filling algorithm.[4] This method takes two forms, one is a more heuristic approximation which involves the determination of a coarse-grained temperature-dependent activation barrier, $\bar{Q}(T)$, just discussed. In terms of the activation barrier $\eta(T)$ is written as

$$\eta(T) = \eta_o \exp[\bar{Q}(T)/k_B T], \tag{2}$$

where the prefactor η_o will be fixed by taking the high-temperature limit and matching η_o to a value that can be computed using MD. See Ref. 4 where this procedure was carried out for a binary Lennard-Jones model potential. Equation (2) is a familiar expression frequently used to fit or correlate experiment data, therefore obtaining the activation barrier.[17,18] We use this expression differently. We use Eq. (2) to predict the temperature variation of $\eta(T)$ with $\bar{Q}(T)$ already determined, and test the results against experimental measurements. There is another part of our method which is a more rigorous formulation of viscosity calculation, based on the Green–Kubo formalism. Instead of using MD to evaluate the integral of the stress correlation function, we introduce a Markov network model to utilize the information provided by the TSP trajectory sampled by our algorithm.[19] This method has been applied to the BLJ system;[4] further details of its implementation will be reported separately.[19]

We now compare three types of viscosity results on silica, all displayed in Fig. 6. All results are shown in absolute viscosity units and the temperature in °K. First we have the calculations using the Green–Kubo formula and MD simulations which are reliable but exist only in the low-viscosity region. Then we have experimental measurements which exist only in the intermediate to high-viscosity range. Lastly, results of the present method, which we will denote as the SAP approximation, extend over the entire range of values, and overlap with both the MD results and the experiments. Looking first at the low-viscosity region, below $\eta \sim 1$ Pa s, two sets of MD results are shown. The two lowest data points (open circles) are our own calculations using
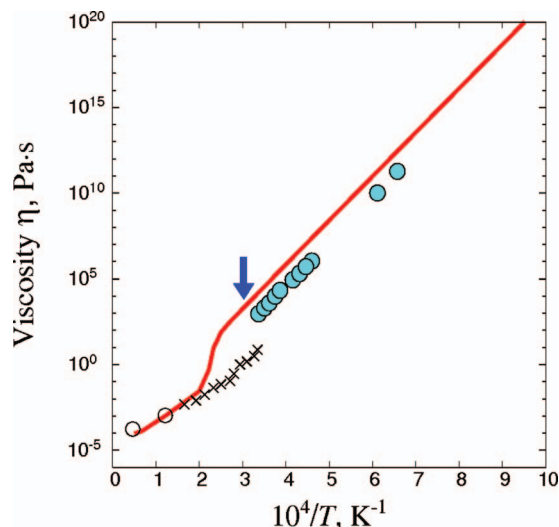
FIG. 6. Viscosity of SiO_2, calculation using transition state theory and the activation barrier in Fig. 5(b) (solid line), experimental data (filled circles) (Ref. 16), our NEMD results (open circle), and MD simulation results (crosses) (Ref. 15). Arrow indicates a crossover between fragile and strong behavior suggested from simulations of entropy and diffusivity in a model silica (Ref. 23).

FIG. 7. Activation process with (a) high and (b) low Q at α and β indicated in Fig. 5(b). Both high and low Q process involves local rearrangement of Si–O bond.

a nonequilibrium molecular dynamics (NEMD) method.[20] These NEMD viscosity points are used to set the prefactor η_o in Eq. (2). The other 11 data points (crosses) are the results of a large-scale MD simulation by Horbach and Kob[15] using a more sophisticated silica potential model[21] than the present work. These may be considered the most accurate MD results available on silica.

In the low-viscosity region we see a good match between NEMD and the first five MD points. This suggests the effects of different potentials are not significant at very low viscosities, $\eta \lesssim 10^{-3}$ Pa s. We also see that SAP results, based on activated state kinetics through $\bar{Q}(T)$, are consistent with the totally independent MD results out to the first five points. We take this to be a measure of validation of the present approach, although in a limited temperature range. The next six viscosity points from MD simulation show a discernible change in slope relative to the first five points, occurring around 4000 °K. While the possible significance of this feature was not discussed originally,[15] we can now give this a new interpretation, a crossover from strong-to-fragile behavior, as suggested by the SAP result. We will return to this point below after considering the intermediate and high-viscosity portions of Fig. 6.

The more critical test of our method is in the high-viscosity range, 10^2–10^{12} Pa s. As shown in Fig. 6 we have a direct comparison between the SAP results and experiment. An Arrhenius temperature variation is well predicted, while a systematic overestimate of the viscosity magnitude is seen. The latter is actually expected from the way the activation barrier $\bar{Q}(T)$ was obtained (see Sec. III), as a similar behavior was also found in the SAP results for a fragile liquid.[4] From the SAP results we obtain the glass transition temperature T_g to be 1580 K, defined by $\eta(T_g) = 10^{12}$ Pa s, which may be compared to the experimental value of 1446 K.[16] Again, the higher T_g should be attributed to the SAP approxi-
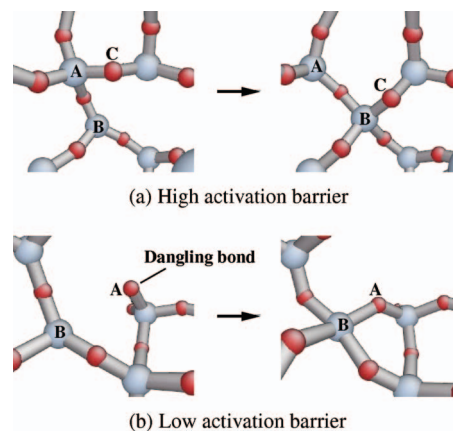
mation which is an upper-bound estimate. We can expect the results from the network model[19] to give lower viscosities and a lower value of T_g. From the experimental viscosity data one finds the activation energy to be 5.33 eV.[22] In our independent determination using TSP trajectory the value we obtain is 5.27 eV, as can be seen in Fig. 5(b).

In the intermediate viscosity range, 10^{-4}–10^2 Pa s, the SAP results show a smooth transition between the portion that overlaps with the NEMD and MD (first five points) calculations and the portion that spans the experimental data. We interpret this as two closely spaced crossovers. As the viscosity increases with decreasing temperature, one encounters a first transition, which we can call the high-temperature crossover, from strong to fragile, followed by a second transition, the low-temperature crossover, from fragile to strong. In this context, the MD results (next six points) may be an indication of the high-temperature crossover. On the basis of atomistic calculations of entropy and diffusion coefficient using the same potential as the MD simulations,[15] a low-temperature crossover at 3300 K has been proposed.[23] This is shown by the arrow in Fig. 6. At this point we cannot be too definitive about the supporting evidence for our SAP results showing two crossovers. We will see below that combining the results for silica with those for the binary Lennard-Jones potential model leads quite naturally to a scenario where two crossovers are expected in all viscous liquids.

In our study of fragile behavior,[4] analysis of the atomic configurations associated with specific activation events has revealed interesting details of atomic rearrangements. The corresponding results for SiO_2 are shown in Fig. 7. We find two mechanism characteristics of network-structure systems, a bond switching process associated with high barriers, and another process at low barriers activated by the presence of dangling bonds. As illustrated in Fig. 7(a), at high Q, indicated by α in Fig. 5(b), the Si–O bond AB breaks while a new bond BC is formed. Figure 7(b) shows that at low Q, see β in Fig. 5(b), a nonbonding O atom A binds with a Si atom B to form a Si–O bond AB. Regardless of the activation energy all activation processes are local bond rearrangements involving only a few atoms. Additionally, atoms participating in bond rearrangements at low activation are either under- or overcoordinated.
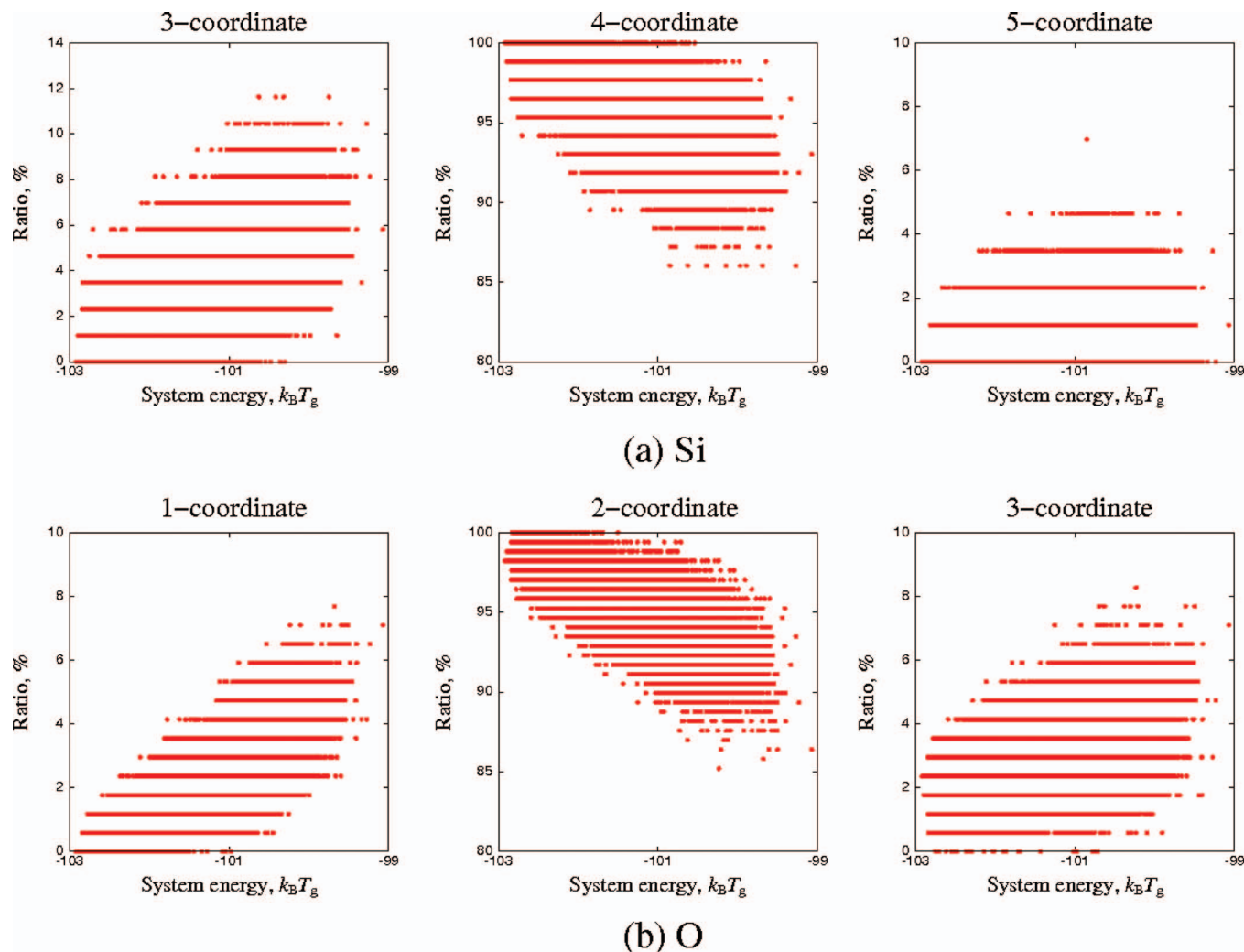
FIG. 8. Distribution of percentage of (a) Si atoms with three-, four-, and five-coordinated atoms and (b) O atom with one-, two-, and three-coordinated atoms at different inherent structure minima. Low energy minima have larger number of perfect coordinated atoms while high energy ones have more over- or undercoordinated atoms.

Further insight into the temperature dependence of activation barrier may be gained by considering the local bond orders. Each panel in Fig. 8 shows the inherent structure energy distribution of the fraction of Si and O atoms that are three-, four-, and fivefold coordinated. Here atom pairs with distance less than 0.25 nm are defined as bonded atoms, a criterion established from an analysis of the radial distribution function. Notice that the fraction of perfectly coordinated (four-coordinate) atoms is greater at lower energies, while the population of under (three)-/over (five)-coordinated atoms is biased toward the high energies. Since inherent structure energies decrease with decreasing temperature, the number of over-/undercoordinated atoms in the system also decreases. The activation barrier therefore should increase with decreasing temperature.

IV. TOWARD A UNIFIED VIEW OF LIQUIDS WITH STRONG AND FRAGILE BEHAVIOR

The combination of our SAP results on a strong liquid with previous results on a fragile system[4] points to a unifying interpretation of fragility in terms of the coarse-grained temperature-dependent activation barrier $\bar{Q}(T)$. Figure 9 shows the SAP viscosities for silica and the binary Lennard-Jones model, and their corresponding $\bar{Q}(T)$ (inset). Also shown are experimental data (symbols) to indicate the extent to which the two theoretical results can describe the measurements.[16] Assuming for the moment that the theoretical curves are accurate enough, we note that the two activation barriers share a generic structure, as sketched schematically in Fig. 10. The essential features of this generic temperature-dependent activation barrier are two limiting values at low and high T, which we denote as Q_H and Q_L, respectively, and a smooth interpolation in the transition region demarcated by temperatures T_L and T_H, respectively. The physical picture depicted in Fig. 10 is the following. When the system is evolving at temperatures above $>T_H$, it encounters only shallow potential wells and therefore requires only a low activation energy Q_L. However if the system is evolving at temperatures below T_L, it is likely to be trapped in deep potential wells and therefore will require a high activation energy Q_H. Is it reasonable to assume that at lower temperatures, the system will find itself in deeper wells? The answer is yes since lower energy states will be-
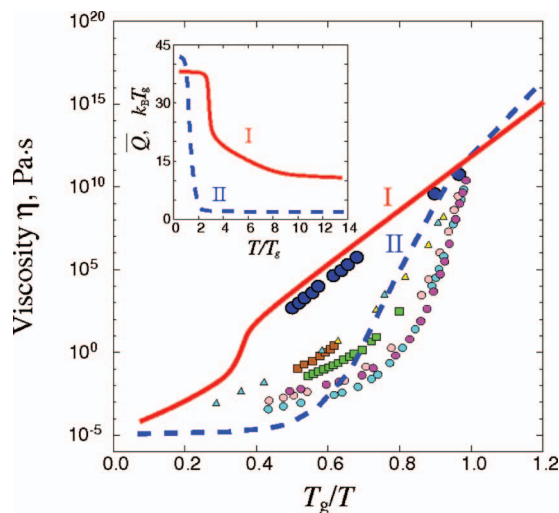
FIG. 9. Comparison of viscosity calculations for SiO_2 and BLJ (Ref. 4) with experimental data on SiO_2 (circles) and fragile glass formers (other symbols) (Ref. 16). The inset shows the coarse-grained activation barriers for the two model systems. SAP formulation results are for SiO_2 (solid curve, labeled I) and BLJ (dashed curve, labeled II).

come increasingly favorable at lower temperatures. This can be seen directly by the results in Fig. 2. The temperature variation of the generic barrier, $Q(T)$, in Fig. 10 is merely an interpolation between its two limiting values. Notice that any method that can determine $Q(T)$ is sufficient to fix the set of four physical parameters (Q_H, Q_L, T_H, and T_L). The transition range, between T_L and T_H, may be regarded as the *fragility zone*. Outside of this range, $Q(T)$ is a constant. With the help of Fig. 10 one can readily appreciate the commonality between a strong and a fragile liquid, and by extension their respective viscosities in Fig. 9. In the particular case of SiO_2 and BLJ, we see that the high activation barrier magnitudes are similar, Q_H, $\sim 40-50 k_B T_g$, whereas the low activation barriers are quite different, $Q_L \sim 10 k_B T_g$ (SiO_2) versus $2 k_B T_g$ (BLJ). Since Q_H (Q_L) governs the slope $d\eta/dT$ at T_H (T_L), this effect can be seen in Fig. 9. The large difference in Q_L also leads to an appreciable difference in the extent of the fragility zone, smaller for SiO_2 than for BLJ, which in turn explains the pronounced fragile behavior of the latter. To explain why Q_L is so much larger for SiO_2 than BLJ, one can
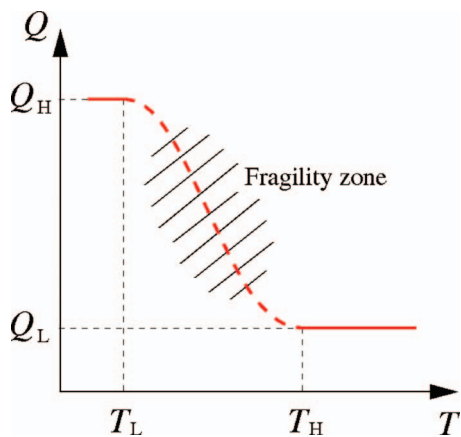

FIG. 10. Schematic of an activation barrier with a two-level structure.

return to examine the activation mechanism discussed in Fig. 7(b) and compare it with the corresponding mechanism for BLJ discussed previously.[4]

A direct consequence of Fig. 10, self-evident by inspection, is the existence of two transitions between strong and fragile behavior. As a system starting out at a high temperature, above T_H, its viscosity behavior should be strong since Q is a constant. As T crosses below T_H, a crossover to fragile behavior should occur. With further temperature decrease the system maintains its fragile behavior until T crosses T_L, at which point a second crossover to strong behavior should set in. Thus, two crossovers should be a universal feature of all glass formers.

V. PES TOPOGRAPHY: LANDSCAPE ROUGHNESS

We have taken advantage of having results for a strong and a fragile liquid in a comparable form to discuss their commonality. These results are also useful for pointing out the distinguishing features of each liquid.[16] We now examine the extent to which strong and fragile liquids differ in the topography of their potential energy landscapes.

The topological characteristics of a multidimensional PES can be explored through various measures. One approach is to map the configuration space into multiple minima and transition states (barriers or saddle points) connecting these minima in the form of "disconnectivity graphs."[24,25] This is a way to describe the general shape and overall connectivity that define the system landscape. We have previously produced such a graph for the BLJ model to display the characteristics of a fragile system.[4] In Fig. 11 we compare this result with the corresponding graph for SiO_2, as derived from the TSP trajectory results of Fig. 3. Each local minimum is indicated by the end point of a vertical line while a saddle point (transition state) is denoted by a vertex. The graph for a fragile system displays a multitude of splitting, strong fluctuations in depth of local minima, and significant basin connectivity, features that give the appearance of a "willow tree" in analogy with tree diagrams.[25] None of these features are evident in the graph for SiO_2. Generally speaking PES structures may be classified as rough, single minimum, and funnel.[24] Each is associated with a distinctive disconnectivity graph, and a corresponding schematic of a one-dimensional cut of the $3N$-dimensional PES. The latter, in particular, is a useful representation for visualizing and comparing different physical systems. From the graphs of Fig. 11 we have deduced the corresponding schematic potential profiles shown in Fig. 12. We see that the profile for SiO_2 may be described as a broad-base funnel with relatively small fluctuations in depth of the local minima, with an overall "smooth" appearance. This is in contrast to the profile for BLJ which indeed shows the features expected of a rough energy landscape. It is worth noting that the landscape profiles in Fig. 12 are systematically deduced from quantitative data that are interatomic potential specific, from the TSP trajectory (Fig. 3) to the disconnectivity graphs (Fig. 11). Such comparisons provide a semiquantitative way of relating system specifications at the level of ineratomic potential and
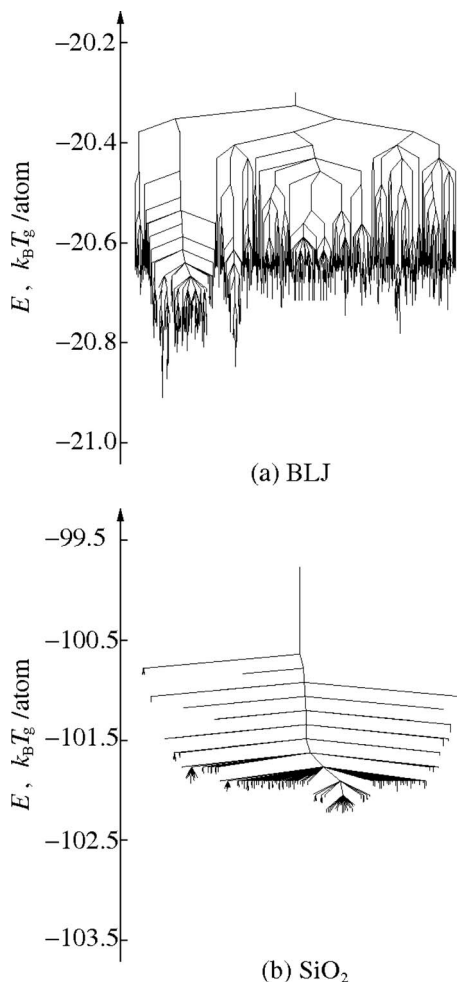
(a) BLJ

(b) SiO$_2$

FIG. 11. Disconnectivity graphs of (a) BLJ and (b) SiO$_2$ constructed from their respective TSP trajectories.

(a) BLJ

(b) SiO$_2$

FIG. 12. Potential energy landscape profiles for (a) BLJ and (b) SiO2, obtained by taking one-dimensional cuts across the disconnectivity graphs shown in Fig. 11.

calculated activation barrier to a physical property, the viscosity. Figures 11 and 12 may be considered as contributing to the continuation of ongoing discussions on distinctive landscape features of strong and fragile liquids.[16,26,27]

VI. DISCUSSION

This work is a continuation of our study of the viscosity of a viscous liquid as it is cooled toward its glass transition temperature. Our purpose here is twofold. The first is to test the atomistic approach, previously applied to a model fragile system,[4] on a model of SiO$_2$, well known for its opposite limiting behavior. Using the same method we generated TSP trajectories, performed activation barrier analysis, and obtained viscosity results that compare well with experiment (see Fig. 6). A second purpose is to compare the silica and BLJ model results, calculated consistently using the same methods for two different interaction potentials, to identify both common and distinguishing features. In terms of the effective temperature-dependent activation barrier we find all viscous liquids should display two crossovers between strong and fragile behaviors. We also find that the atomic rearrangements associated with activation events are quite different for strong and fragile liquids, and there is a quantifiable
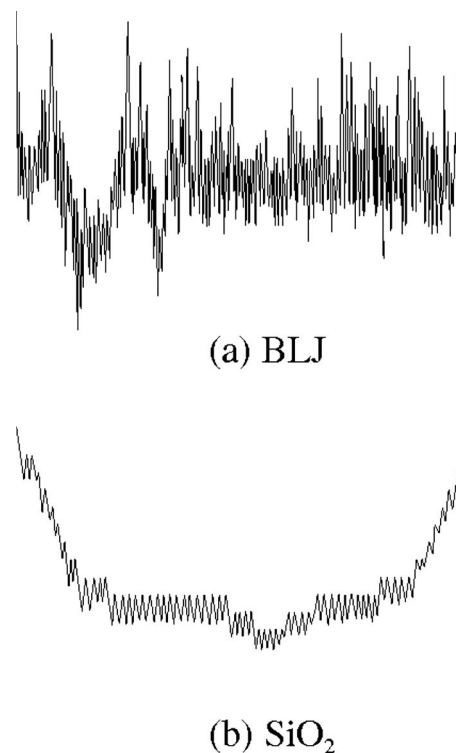
difference in the topographic connectivity (see Fig. 11) and the roughness of the one-dimensional schematic potential energy profile (Fig. 12).

Our results thus point to the fundamental nature of fragile and strong behaviors in viscosity. As suggested by our abstraction of the coarse-grained temperature-dependent activation barrier (Fig. 10), all liquids in their supercooled states should have a "fragility zone" connecting two regions in which the barriers have significantly different magnitudes, but both are essentially temperature insensitive. As a consequence, the viscosity variation should show two transitions as the liquid is cooled below the melting point, strong to fragile first, followed by fragile to strong.

Since the temperature variation of the viscosity has been a central issue in discussions of the glass transition,[1–3,5,16,26,27] our atomistic calculations lend further insight into the mechanisms of structural relaxation in the two prototypical systems. Additionally, disconnectivity graphs and the schematic potential profiles derived from them provide topological and connectivity characteristics to quantify our notions of a "rough" energy landscape associated with fragile glass formers.

Two aspects of our study deserve further attention. One is an improvement to our single relaxation path approximation. This can be addressed by including coupling effects between deep basins.[19] The other is to extend our viscosity calculation to the high-temperature region where linear response theory and MD simulation become applicable. Results on both investigations will be reported.

ACKNOWLEDGMENTS

[1] C. A. Angell, Science **267**, 1924 (1995).

[2] J. C. Dyre, Rev. Mod. Phys. **78**, 953 (2006).

[3] K. Trachenko and V. V. Brazhkin, J. Phys.: Condens. Matter **20**, 075103 (2008).

[4] A. Kushima, X. Lin, J. Li, J. Eapen, J. C. Mauro, X. Qian, D. Phong, and S. Yip, J. Chem. Phys. **130**, 224504 (2009).

[5] F. H. Stillinger, Science **267**, 1935 (1995).

[6] C. A. Angell, J. Phys. Chem. **97**, 6339 (1993).

[7] B. P. Feuston and S. H. Garofalini, J. Chem. Phys. **89**, 5818 (1988).

[8] S. Andersson and L. Dzhavadov, J. Phys.: Condens. Matter **4**, 6209 (1992).

[9] F. H. Stillinger and T. A. Weber, Phys. Rev. A **25**, 978 (1982).

[10] J. C. Mauro, R. J. Loucks, J. Balakrishnan, S. Raghavan, J. Chem. Phys. **126**, 194103 (2007).

[11] S. Sastry, Nature (London) **409**, 164 (2001).

[12] D. A. McQuarrie, *Statistical Mechanics* (Harper & Row, New York, 1973), p. 512.

[13] J.-P. Hansen and I. R. MacDonald, *Theory of Simple Liquids* (Academic, London, 1976).

[14] G. A. Fernandez, J. Vrabec, and H. Hasse, Fluid Phase Equilib. **221**, 157 (2004).

[15] J. Horbach and W. Kob, Phys. Rev. B **60**, 3169 (1999).

[16] C. A. Angell, J. Phys. Chem. Solids **49**, 863 (1988).

[17] S. G. Brush, Chem. Rev. (Washington, D.C.) **63**, 913 (1962).

[18] D. Kivelson, G. Tarjus, X. Zhao, and S. A. Kivelson, Phys. Rev. E **53**, 751 (1996).

[19] J. Li, see: http://mt.seas.upenn.edu/Stuff/vis/Notes/main.pdf.

[20] F.-M. Plathe, Phys. Rev. E **59**, 4894 (1999).

[21] B. W. H. Van Beest, G. J. Kramer, and R. A. van Santen, Phys. Rev. Lett. **64**, 1955 (1990).

[22] G. Urbain, Y. Bottinga, and P. Richet, Geochim. Cosmochim. Acta **46**, 1061 (1982).

[23] I. Saika-Voivod, P. H. Poole, and F. Sciortino, Nature (London) **412**, 514 (2001).

[24] O. M. Becker and M. Karplus, J. Chem. Phys. **106**, 1495 (1997).

[25] D. J. Wales, Int. Rev. Phys. Chem. **25**, 237 (2006).

[26] F. H. Stillinger, J. Chem. Phys. **88**, 7818 (1988).

[27] J. C. Mauro, R. J. Loucks, A. K. Varshneya, and P. K. Gupta, Sci. Model. Simul. **15**, 241 (2008).